RSC Advances

PAPER

View Article Online
View Journal | View Issue

Cite this: *RSC Adv.*, 2020, **10**, 1769

Effects of metal–organic complex Ni(Salen) on thermal decomposition of 1,1-diamino-2,2-dinitroethylene (FOX-7)†

Wenzhe Ma, ‡[ab] Yanjing Yang, ‡[a] Fengqi Zhao,*[a] Kangzhen Xu,*[b] Jiankan Zhang,[a] Ming Zhang[a] and Zhicun Feng[b]

The development of novel combustion catalysts is critical for improving combustion performance of high-energy solid propellants. In this work, a nickel-based Schiff base complex, *N*,*N*′-bis(salicylidene) ethylenediamino nickel [Ni(Salen)], as a candidate for the combustion catalyst of solid propellants, was synthesized with high purity. The effects of Ni(Salen) on the thermal decomposition reaction of FOX-7, which is closely related to its combustion properties in propellants, were systematically investigated and the corresponding mechanisms were also evaluated through comparison and analysis. Under the action of Ni(Salen), peak temperatures of the two decomposition processes of FOX-7 were reduced from 235.7 and 296.3 °C to 233.7 and 268.7 °C, respectively. The investigations into the mechanisms revealed the interactions between the Schiff base skeleton in Ni(Salen) and FOX-7, which promotes the decomposition of the remaining FOX-7. In addition, it was found that NiO, which was a decomposition product of Ni(Salen), also played an important role in promoting the thermal decomposition of FOX-7.

Received 31st October 2019
Accepted 28th December 2019

DOI: 10.1039/c9ra08973j

rsc.li/rsc-advances

1. Introduction

The investigation of high-performance solid propellant is critical for development of advanced solid rockets for both civil and military applications.[1–3] Recently, the research of solid propellants with lower impact sensitivities has attracted great attention due to their favorable safety, which is essential for the novel advanced solid rockets.[3–5] 1,1-Diamino-2,2-dinitroethylene (FOX-7, $C_2H_4O_4N_4$) (Fig. 1a) is a novel energetic material with good thermal stability and low impact sensitivity, thus making it the most promising candidate as the energetic component of insensitive propellants.[6–12] The combustion performance of solid propellants, including burning rates, pressure exponents and temperature coefficient, are significant for the performance of the corresponding solid rocket engines.[1,3,13] The addition of combustion catalysts is an effective approach to adjust the combustion performance.[14–16] Moreover, it is well-known that the thermal decomposition properties of energetic compounds are closely related to their combustion properties in propellants.[17,18] Many researchers have demonstrated that the lower the decomposition temperatures of energetic materials would lead to the higher the burning rates of propellants.[19] Therefore, the thermal decomposition characteristics of FOX-7, including its decomposition temperatures, activation energy and reaction rates, are believed to have great influences on the combustion properties of FOX-7-containing propellants.[17,20–24] In addition, the development of compounds that could adjust the thermal decomposition behavior of FOX-7 is essential to optimize the combustion properties of solid propellants with FOX-7 as an energetic component.[25–28] In the past two decades, the thermal decomposition of FOX-7 has been extensively studied by taking advantages of the catalytic activity of single-metal oxides and composite oxides, including Fe_2O_3,[29] CuO,[30] MnO_2,[31] V_2O_3 (ref. 32) and $CuFe_2O_4$.[18] Especially, $CuFe_2O_4$ has been found to be able to reduce the peak temperatures of two exothermic decomposition steps of FOX-7 by 14.7 °C and 13.8 °C. Many researches have indicated that in comparison with metal oxides, metal complexes often possess better catalytic effects on the thermal decomposition of energetic materials, including ammonium perchlorate (AP, NH_4ClO_4), cyclotrimethylenetrinitramine (RDX, $C_3H_6N_6O_6$), and 1,3,5,7-tetranitro-1,3,5,7-tetrazocane (HMX, $C_4H_8N_8O_8$).[1,14]

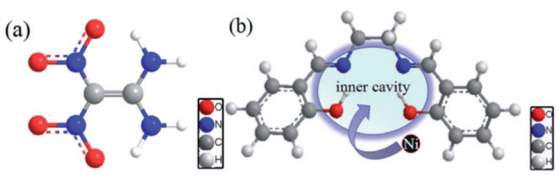

Fig. 1 The structure of FOX-7 (a) and Salen (b).

[a]*Xi'an Modern Chemistry Research Institute, Xi'an, Shaanxi 710065, China. E-mail: zhaofqi@163.com*

[b]*School of Chemical Engineering, Northwest University, Xi'an, Shaanxi 710069, China. E-mail: xukz@nwu.edu.cn*

† Electronic supplementary information (ESI) available. See DOI: 10.1039/c9ra08973j

‡ W. Z. Ma and Y. J. Yang contributed to this work.

The compounds based on the Schiff bases with various structures, possess many interesting properties including catalytic, magnetic and biological properties.[33–38] Specifically, they have been proved to have high catalytic activity in the hydrogenation of cyclohexene reaction, carbene reaction, and nitrogen cycle reaction.[33,39] It is noticed that nitrogen cycle reactions are involved in the thermal decomposition of FOX-7 and the combustion processes of propellants containing FOX-7.[9,12,33] Therefore, the metal Schiff base compounds are proposed to be potential catalysts for enhancing the decomposition and combustion of FOX-7.

N,*N*′-Bis(salicylidene)ethylenediamino (Salen) is a widely used Schiff base which has suitable inner cavity between its two salicylaldehyde structures to accommodate metal ions to form stable metal complexes (Fig. 1b).[40] Studies have shown that nickel-based catalysts can effectively increase the high temperature activity and selectivity of amino groups,[35,39] so it is foreseeable that nickel-based catalysts have important influences on the thermal decomposition behavior of FOX-7. Moreover, studies also have shown that nickel coordination compounds as active ingredients have shown very good application prospects in catalysis and phase stability.[39,41]

In this work, Ni(Salen) was synthesized and selected as a candidate for combustion catalysts of solid propellants and its effects on thermal decomposition of FOX-7 were investigated.

2. Experimental

Caution! FOX-7 is an energetic compound to be sensitive towards impact and friction. When handling FOX-7 and its mixtures with Ni(Salen), proper protective measures including ear protection, Kevlar gloves, face shield, body armor, and earthed equipment should be used.

2.1 Materials

All the chemicals used for the synthesis were commercially available. Salicylaldehyde ($C_7H_6O_2$, 99.5%), ethylenediamine ($C_2H_8N_2$, 99.9%), nickel chloride hexahydrate ($NiCl_2{\cdot}(6H_2O$, 99%) and NaOH were purchased from Aladdin Inc. Distilled water and ethanol (Xi'an Chemical Reagent Factory, 95%) were used for the preparation of samples. FOX-7 was synthesized in our institute (Xi'an Modern Chemistry Research Institute) based on the literature and the purity is over 99%.[9]

2.2 Synthesis of Ni(Salen)

N,*N*′-Bis(salicylidene)ethylenediamino (Salen) was prepared according to ref. 42. Salen (2.68 g, 0.01 mol) was dissolved in ethanol (30 ml) and heated to 55 °C. NaOH solution (35 ml, 6 mol L^{-1}) was gradually added to the Salen solution. Then, ethanol solution of $NiCl_2$ (20 ml, 0.05 mol L^{-1}) was added dropwise. After stirring for 2 h, the precipitates with blood red color appeared. The precipitates were filtered, washed with ethanol and water and dried to obtain the final product Ni(Salen) complex. Yield: 82.5%. Elem. anal. (%). Calcd for $C_{16}H_{14}N_2NiO_2$: C, 59.13; H, 4.34; N, 8.62. Found: C, 59.73; H, 4.31; N, 8.54.

Single crystals for the Ni(Salen) complex were obtained by the solvent evaporation method at ambient temperature.

2.3 Characterization

Elemental analysis (C, H, N) was performed by the combustion method on a Flash EA 1112 full-automatic trace element analyzer, and the amount of each test was 7.00 mg. Its accuracy is better than 0.5%.

Phase identification was conducted using powder X-ray diffraction (XRD) on a PANalytical X'Pert Pro X-ray Diffractometer with Cu Kα radiation ($\lambda = 1.5418$ Å) at 40 kV and 40 mA. The data were collected from 5° to 90° (2θ) in steps of 0.05° at ambient temperature.

The vibrational characteristics of chemical bonds were determined using a Bruker Tensor 27 Fourier Transform Infrared (FT-IR) spectrometer. The spectra of the samples (as KBr pellets with a KBr to sample mass ratio of approximately 30 : 1) were acquired in the range of 4000–400 cm^{-1} in transmission mode with a resolution of 2 cm^{-1}.

The morphology and the microstructures of the metal complexes and the ligand were studied by field emission scanning electron microscope (FESEM) of Zeiss SIGMA. The sample is enlarged 1000 times to get high-definition picture.

The DSC experiments were performed using a DSC200 F3 apparatus (NETZSCH, Germany) under a nitrogen atmosphere at a flow rate of 80 ml min^{-1}, and the heating rates were 10.0 °C min^{-1} from ambient temperature to 350 °C. In addition, unless otherwise noted, the mass ratio of the mixture samples for the DSC tests is 1 : 10 [Ni(Salen) : FOX-7]. The TG/DTG experiment was performed using SDT-Q600 apparatus (TA, USA) under a nitrogen atmosphere at a flow rate of 100 ml min^{-1}, and the heating rate was 10.0 °C min^{-1} from ambient temperature to 500 °C.

X-ray photoelectron spectroscopy (XPS) analysis was conducted on an ESCALAB 250 Xi XPS microprobe (Thermo Scientific, UK). The sample was prepared by sprinkling powder on a carbon tape attached to the sample holder. XPS spectra were recorded using monochromatic Al-Kα (186.6 eV) X-ray sources under an ultimate pressure of 5×10^{-10} mbar. All data were calibrated using the adventitious C 1 s signal at 284.8 eV as a reference.

3. Results and discussion

3.1 Crystal and structure of Ni(Salen)

The XRD pattern of the as-prepared Ni(Salen) complexes was obtained and compared with the pure Salen ligand (2θ from 5° to 80°). As shown in Fig. 2a, no diffraction peaks belonging to Salen are observed on the XRD pattern of Ni(Salen), indicating that there is no Salen left in the as-prepared sample. The new peaks at 6.68°, 12.79°, 13.79°, 14.56°, 17.78°, 18.67°, 20.57°, 24.57°, and 27.12°detected on the pattern are attributed to Ni(Salen), which fits well with the literature, confirming the successful synthesis of this compound and its high purity.[42,43] In addition, the high signal-to-noise ratio of the XRD pattern suggests the good crystallinity of Ni(Salen).

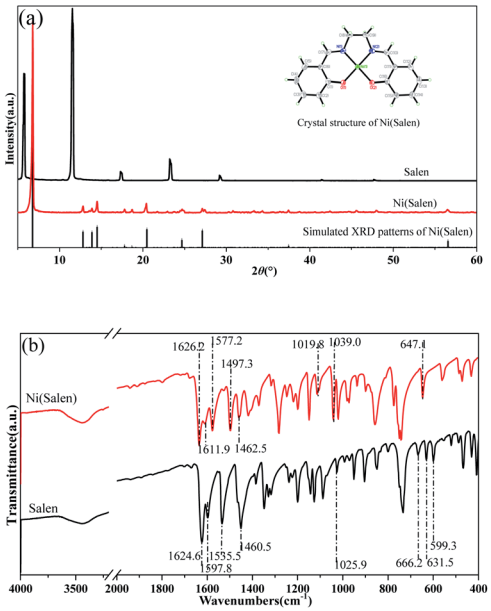

Fig. 2 (a) XRD pattern and (b) FTIR spectrum of the Salen ligand and Ni(Salen).

The single crystals of Ni(Salen) were also obtained and characterized. X-ray single crystal diffraction studies show that the as-synthesized Ni(Salen) crystallizes in an orthorhombic system with the space group of *Pbca* and contains eight molecules per unit cell, which is consistent with the literature.[42] Based on the structure derived from the X-ray single crystal diffraction data, the X-ray powder diffraction pattern of Ni(Salen) is achieved *via* calculation, and the measured pattern is found to be in good agreement with the simulated pattern (Fig. 2a). This result further confirms the preparation of high-purity Ni(Salen) samples.

The structural characteristics of Ni(Salen) were further investigated by using FTIR. As shown in Fig. 2b, two stretching vibrational absorption bands of the bridged carbon–nitrogen double bond (1462.5 cm^{-1}) and the carbon–nitrogen single bond (1624.6 cm^{-1}) are detected both on the spectra of Salen and Ni(Salen), indicating that the bridging ethyl did not participate in the coordination. On the other side, the two absorption peaks belonging to the phenolic hydroxyl group at 1019.8 cm^{-1} and 1039.0 cm^{-1} in Salen merge into to one (1025.9 cm^{-1}) in the complex, and this is attributed to the coordination of –OH with the Ni^{2+} ion. Moreover, the absorption peaks appearing at 666.2, 631.5, and 599.3 cm^{-1} are attributed to the Ni–O coordination bonds, which suggests that the transition metal in the complex is coordinated with the phenolic hydroxyl group. The coordination structure derived from the above FTIR characteristics is in good coincidence with the crystal structure reported in the literature.[38] In addition, it is noticed that, three absorption bands belonging to the benzene ring (1611.9, 1577.2, 1497.3 cm^{-1}) are observed on the Salen spectrum, whereas only two bands (1597.8, 1535.5 cm^{-1}) are present on the spectrum of Ni(Salen). The reason for the phenomenon is that, the electron donor capacity of oxygen atoms of the phenolic hydroxyl group to the benzene ring is increased due to the existence of Ni, thus leading to the changes in the position and number of absorption peaks of the carbon frame.

3.2 Effects of Ni(Salen) on thermal decomposition of FOX-7

The thermal behaviors of FOX-7 and Ni(Salen) were also recorded for comparison. As shown in Fig. 3a, the thermal decomposition curve of FOX-7 showed an endothermic peak at 115.9 °C due to its phase transition. Upon further heating, the pristine FOX-7 decomposes *via* two stages, *i.e.* the relatively slow exothermic decomposition with peak temperature (T_p) at 235.7 °C and the intensive exothermic decomposition with T_p at 296.3 °C. According to the literature,[10,11] the first-stage decomposition of FOX-7 is the denitrification process, and the second one is the formation of HONO due to the break of the second nitro, which causes the entire molecule to completely decompose. The as-prepared Ni(Salen), it is interesting to find that no significant thermal effects appear during thermal decomposition except for an endothermic peak at 126.5 °C belonging to phase transition. As for the FOX-7/Ni(Salen) mixture (Ni(Salen) : FOX-7 = 1 : 10), FOX-7 in the mixture still shows two-stage thermal decomposition behavior, suggesting that the decomposition mechanism of FOX-7 may not be altered. The peak temperatures for the first and second decomposition stages are determined to be 233.7 °C and 268.7 °C for the mixture, respectively. In comparison with the pure FOX-7, the peak temperatures of the FOX-7 in mixture were decreased by 2 °C and 27.8 °C for the first and second stages, respectively. Obviously, Ni(Salen) is very effective in promoting the thermal

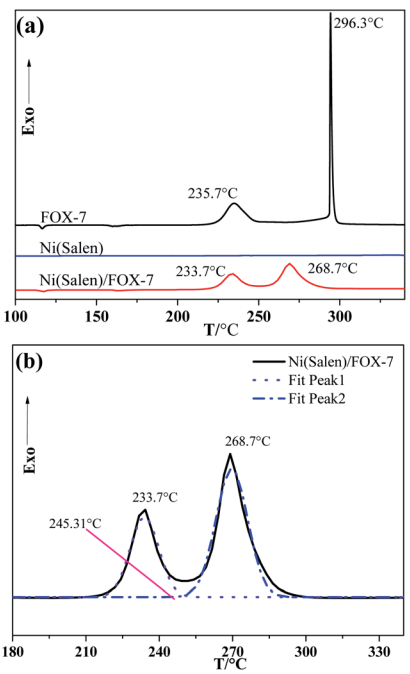

Fig. 3 (a) DSC curves of FOX-7, Ni(Salen) and FOX-7/Ni(Salen) mixtures; (b) DSC curves of FOX-7/Ni(Salen) mixtures from 180 to 340 °C.

decomposition of FOX-7, especially the second-stage decomposition. In addition, it is noticed that in the existence of Ni(Salen), the second thermal-decomposition stage of FOX-7 initiates at about 245.31 °C at which the first one has not been finished (Fig. 3b).

TG tests were also performed to further understand the decomposition processes of FOX-7/Ni(Salen) mixtures (Ni(Salen) : FOX-7 = 1 : 10). As shown in Fig. 4, upon heating, two-stage mass-loss behavior is observed for the pristine FOX-7, which fits well with the DSC results, confirming the two exothermic stages of decomposition reactions. For the Ni(Salen), although no obvious thermal effects were detected in the DSC measurement, its decomposition is found to initiate at about 300 °C and peaked at 373.3 °C with a mass loss of 38.12%. It is noticed that the thermal-stability of Ni(Salen) is higher than that of FOX-7. As for the FOX-7/Ni(Salen) mixture, the decomposition initiates at 211.6 °C, and the two-stage decomposition behavior is also detected. The peak temperatures were determined to be 233.7 °C and 268.7 °C for the first and second reaction stage, respectively. It should be noted that no mass losses exist at temperatures higher than 300 °C, indicating that there are interactions between FOX-7 and Ni(Salen) in the thermal decomposition of the mixture, and all the Ni(Salen) is consumed in the interactions. Therefore, the reactions occurring in the temperature range of 200–300 °C should be attributed to the interactions between FOX-7 and Ni(Salen), which is responsible for the enhancement of FOX-7 decomposition.

3.3 Mechanisms of the promoted FOX-7 decomposition

The effects of Salen ligand and Ni^{2+} in Ni(Salen) on the decomposition of FOX-7 were both examined to disclose the role of Ni(Salen) during thermal decomposition of the FOX-7/Ni(Salen) system. The as-prepared Salen was mixed uniformly with FOX-7 at different mass ratios (Salen : FOX-7 = 1 : 10, 1 : 5, 1 : 1, 2 : 1), and then subjected to DSC thermal analysis. The results are shown in Fig. 5. For the mixture at the mass ratio of 1 : 10, two exothermic events peaked at 233.8 °C and 273.5 °C are observed, which indicates that the Salen ligand is effective

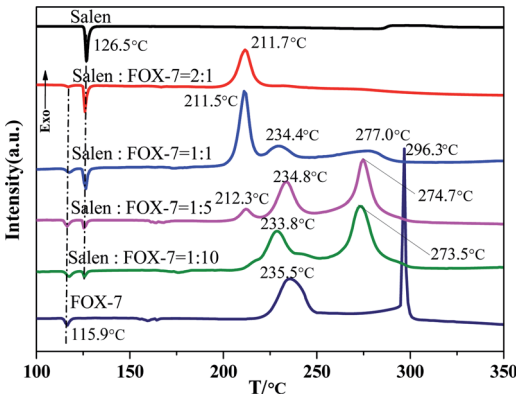

Fig. 5 DSC curves of FOX-7/Salen mixture at different mass ratios, FOX-7 and Salen ligand.

in promoting the second-stage decomposition of FOX-7. For the mixture with a mass ratio of 1 : 5, although similar thermal behavior is observed, a new exothermic peak at 212.3 °C appears on the DSC curve in comparison with the sample with a mass ratio of 1 : 10. Upon further increase of the ratio to 1 : 1, the peaks near 234 °C and 275 °C become weaker, whereas the peak at 211.5 °C is evidently enhanced. Moreover, at a higher mass ratio of 2 : 1, only the exothermic peak at 211.7 °C was detected. The peak near 211 °C is attributed to the interactions between FOX-7 and the ligand Salen. On the other side, the two peaks near 234 °C and 275 °C may originate from the enhanced FOX-7 decomposition. In addition, based on the interaction characteristics stated above, it is proposed that the reaction products between Salen and FOX-7 would promote the thermal decomposition of the remaining FOX-7 and lead to reduced decomposition temperatures. Therefore, Salen as a precursor of an organic active material can promote the second-stage thermal decomposition process of FOX-7, which can evidently influence the decomposition of FOX-7.

A comparison was made between the decomposition behavior of the FOX-7/Ni(Salen) system and the FOX-7/Salen system both with mass ratios of 10 : 1. As shown in Fig. 6, interestingly, it is noticed that the peak temperatures of the

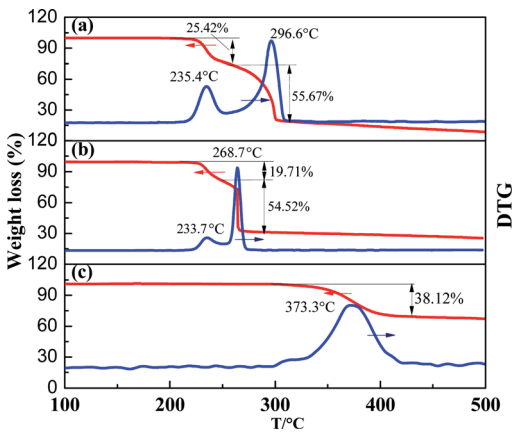

Fig. 4 TG-DTG curves of FOX-7 (a), FOX-7/Ni(Salen) mixture (b) and the Ni(Salen) (c).

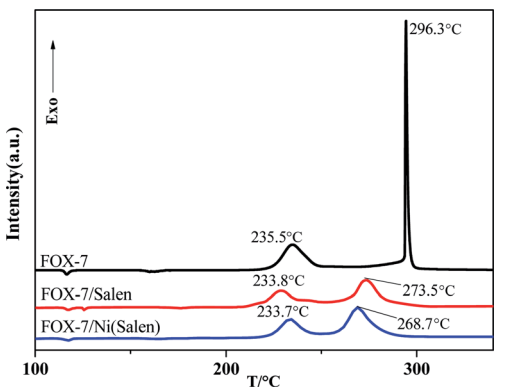

Fig. 6 Different promotion effects of Salen and Ni(Salen) on FOX-7 decomposition.

first-step decomposition are close for both systems. However, for the FOX-7/Ni(Salen) system, the second-step decomposition is peaked at lower temperature than the FOX-7/Salen system. Considering the same contents of the additives and the higher content of Salen ligand in the FOX-7/Salen system, apparently, Ni(Salen) possesses higher activity than Salen in promoting the second-step decomposition of FOX-7. There are two possible reasons behind this: first, Ni^{2+} is also active in enhancing the second decomposition step of FOX-7; second, the existence of Ni^{2+} results in the alteration of the electronic structures of the Salen ligand, thus enhancing activity.

On the other hand, for the purpose of understanding the role of Ni^{2+} in Ni(Salen), nano Ni and nano NiO were added to FOX-7, and the thermal decomposition behavior of the mixtures (Ni/NiO : FOX-7 = 1 : 10) were recorded. The selection of nano Ni and nano NiO is because according to the literatures,[41] nano metal or nano metal oxide particles form in the decomposition of metal complexes. As shown in Fig. 7, when compared with the pure FOX-7, the DSC result of the FOX-7/Ni mixture indicates that the metallic Ni shows no effects on the decomposition of FOX-7. On the other hand, upon the addition of NiO, the peak temperatures of both the first and second decomposition stages are decreased, confirming that Ni^{2+} is able to promote the both decomposition processes of FOX-7 significantly. Therefore, NiO as the decomposition product of Ni (Salen), can significantly promote the two decomposition stages of FOX-7 compared with Ni. For the first step, the peak temperature is decreased by 6.3 °C from 235.7 °C to 229.4 °C. As for the second decomposition step, the peak temperature is reduced by 4.7 °C from 296.3 °C to 291.6 °C. On the basis of the above results, it is proposed that Ni^{2+} is responsible for the enhanced first-step decomposition of the FOX-7/Ni(Salen) system. As for the second step, on the other hand, both Ni^{2+} and the ligand Salen contribute to decreasing the decomposition temperatures.

The FOX-7/Ni(Salen) system (Ni(Salen) : FOX-7 = 1 : 10) was heated to 233 °C and 320 °C and held until the reaction was completed, thus the decomposition products of the first and second step were obtained. The products were subjected to XPS measurements to determine the chemical states of Ni. As exhibited in Fig. 8, for the products of the first decomposition step, the fitted peaks at 853.71 and 870.04 eV are assigned to NiO, and the peaks with binding energy of 857.18 and 874.55 eV are assigned to Ni. In addition, two satellite peaks belonging to NiO were also detected at 860.87 and 878.17 eV. The areas of the peaks assigned to Ni and NiO were also calculated to achieve their contents (listed in Table 1). It is found that the products of the first decomposition step contain 80.71% of NiO and 19.29% of metallic Ni. As for the products obtained at 320 °C, the chemical states of Ni are different. The peaks at 852.38 and 869.62 eV belong to NiO, and the peaks with binding energies of 853.8 and 871.1 eV are assigned to Ni. The peaks with binding energy of 859.3 and 876.5 eV were also attributed to two vibrational companion peaks of Ni (denoted as "Sat"). The calculation indicates that there are 72.04% of Ni and 27.96% of NiO in the products obtained at 320 °C. On the XRD pattern of the products collected at 320 °C, only the diffraction peaks belonging to metallic Ni are observed, indicating its good crystallinity (Fig. 9). In addition, since no peaks of NiO are present on the pattern, it is proposed to be amorphous.

Based on the above investigations into the mechanisms, it is believed that in the FOX-7/Ni(Salen) system, upon heating, the interactions between FOX-7 and Ni(Salen) occur first, leading to the formation of NiO and an organic intermediates, which is also generated from the interactions between FOX-7 and Salen. Both the intermediates and NiO contribute to the decreased decomposition temperatures of FOX-7. The favorable thermal

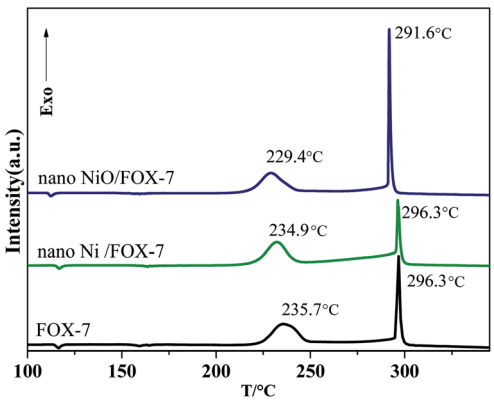

Fig. 7 Different promotion effects of nano NiO and nano Ni on FOX-7 decomposition.

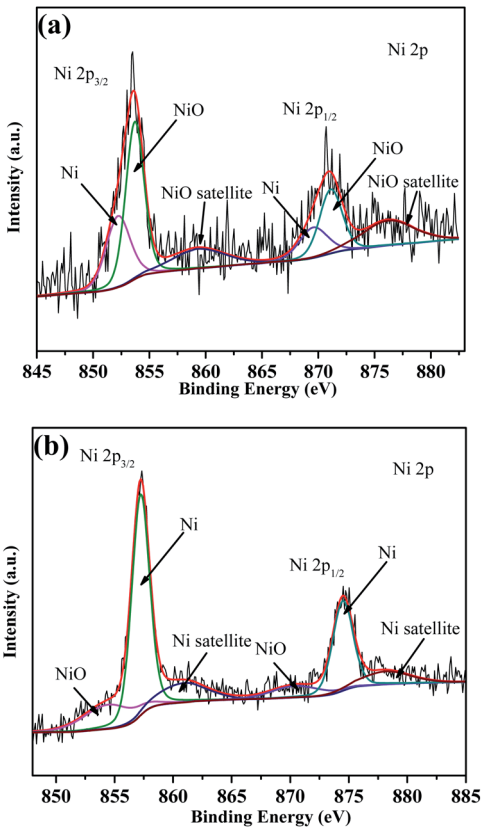

Fig. 8 XPS results of the decomposition products of the FOX-7/Ni(Salen) system collected at 233 °C (a) and 320 °C (b).

Table 1 Ni and NiO contents of the products collected at 233 °C and 320 °C based on the XPS results

Temperature/°C	Ni content/%	NiO content/%
233	19.29	80.71
320	72.04	27.96

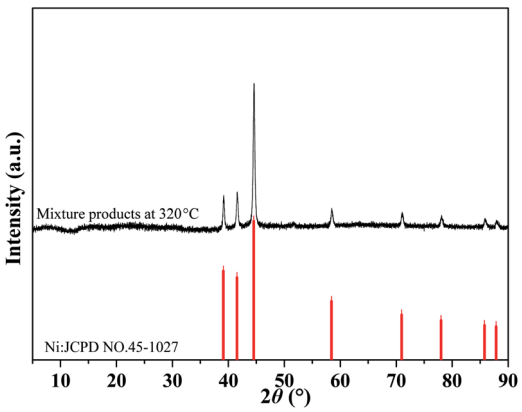

Fig. 9 XRD curves of FOX-7 and Ni(Salen) mixture products heated to 320 °C.

decomposition properties of FOX-7/Ni(Salen) system indicate that the organic ligands with catalytic activity such as Schiff bases are promising for being used to develop novel high-performance combustion catalysts.

4. Conclusions

A compound based on the Schiff base (Salen) was studied as a potential combustion catalyst for insensitive solid propellants containing FOX-7. The addition of Ni(Salen) can significantly change the thermal decomposition processes of FOX-7 and decrease the peak temperatures of the two-stage exothermic decomposition of FOX-7 by 2 °C and 27.6 °C, respectively. The two-step separate decomposition processes are converted into a one-step continuous intense exothermic process, which is advantageous for improving the combustion performance of the FOX-7-containing propellant. The mechanism analysis of the FOX-7/Ni (Salen) system showed that the interactions between FOX-7 and Ni (Salen) first formed NiO and organic intermediates during the heating process. Both the intermediates and NiO contribute to reducing the decomposition peak temperature and improving thermal decomposition performance of FOX-7, which indicates that the catalytically active organic ligands such as Schiff bases are expected to become the development direction of new-type high-performance combustion catalysts.

Conflicts of interest

There are no conflicts to declare.

Acknowledgements

We gratefully acknowledge financial supports received from the National Natural Science Foundation of China (21503163).

References

1 Q. L. Yan, F. Q. Zhao, K. K. Kuo, *et al.*, *Prog. Energy Combust. Sci.*, 2016, **57**, 75–136.
2 B. Gaur, B. Lochab, V. Choudhary and I. K. Varma, *J. Macromol. Sci., Polym. Rev.*, 2003, **43**, 505–545.
3 Y. P. Chai and T. L. Zhang, *J. Solid Rocket Technol.*, 2007, **30**(1), 44–47, 56.
4 H. Wang, F. Q. Zhao and H. X. Gao, *J. Energ. Mater.*, 2005, **13**(5), 344–348.
5 O. P. Korobeinichev, A. A. Paletskii and E. N. Volkov, *Russ. J. Phys. Chem. B*, 2008, **2**, 206–228.
6 W. A. Trzcinski and A. Bellada, *Cent. Eur. J. Energ. Mater.*, 2016, **13**(2), 527–544.
7 U. Bemm and H. Ostmark, *Acta Crystallogr., Sect. C: Cryst. Struct. Commun.*, 1998, **54**, 1997–1998.
8 H. Jiang, Q. J. Jiao and C. Y. Zhang, *J. Phys. Chem. C*, 2018, 1–21.
9 A. J. Bellamy, *Struct. Bonding*, 2007, **125**, 1–33.
10 X. L. Xing, L. Xue, F. Q. Zhao, *et al.*, *Thermochim. Acta*, 2009, **491**, 35–38.
11 M. Anniyappan, M. B. Talawar, G. M. Gore, *et al.*, *J. Hazard. Mater.*, 2006, **B137**, 812–819.
12 K. Z. Xu, Q. Q. Qiu, J. Y. Pang, *et al.*, *J. Energ. Mater.*, 2013, **31**(4), 273–286.
13 Q. L. Yan, S. Zeman, O. J. Šeleš, *et al.*, *J. Therm. Anal. Calorim.*, 2013, **111**, 1419–1430.
14 M. W. Beckstead, K. Puduppakkam, P. Thakre, *et al.*, *Prog. Energy Combust. Sci.*, 2007, **33**, 497–551.
15 B. Florczak, *Cent. Eur. J. Energ. Mater.*, 2008, **5**(3–4), 65–75.
16 G. Singh and S. P. Felix, *Combust. Flame*, 2003, **132**, 422.
17 Y. J. Yang, Y. Bai, F. Q. Zhao, *et al.*, *RSC Adv.*, 2016, **6**, 67308.
18 Y. Zhang, T. T. Wei, K. Z. Xu, *et al.*, *RSC Adv.*, 2013, **1**, 104.
19 F. Yang, D. Deng, X. Pan, *et al.*, Understanding nano effects in catalysis, *Natl. Sci. Rev.*, 2015, **2**(2), 183–201.
20 R. A. Isbell and M. Q. Brewster, *Propellants, Explos., Pyrotech.*, 1998, **23**, 218–224.
21 B. Florczak, *Cent. Eur. J. Energ. Mater.*, 2008, **5**(3–4), 103–111.
22 W. A. Trzciński, S. Cudziło, Z. Chyłek, *et al.*, *37th Int. Annu. Conf. ICT*, Karlsruhe, Germany, June 27–30, 2006.
23 M. M. Mench, C. L. Yeh and K. K. Kuo, *Energetic Materials: Production, Processing, and Characterization*, Fraunhofer-Institut fur Chemische Technologie (ICT), 1998, p. 30.
24 D. M. Badujar, M. B. Talawar, S. N. Asthana, *et al.*, *J. Hazard. Mater.*, 2008, **151**, 289–305.
25 A. A. Said and R. A. Qasmi, *Thermochim. Acta*, 1996, **275**, 83–91.
26 D. V. Survase, M. Gupta and S. N. Asthana, *Prog. Cryst. Growth Charact.*, 2002, **45**, 161–165.
27 W. F. Chen, F. S. Li, J. X. Liu, *et al.*, *Chin. J. Catal.*, 2005, **26**, 1073–1077.

28 Y. P. Tong, Y. P. Wang, Z. X. Yu, *et al.*, *Mater. Lett.*, 2008, **62**, 889–891.
29 E. Alizadeh, B. Shaabani, A. Khodayari, *et al.*, *Powder Technol.*, 2012, **217**, 330–339.
30 X. D. Zheng, P. Li, S. L. Zhen, *et al.*, *Powder Technol.*, 2014, **268**, 446–451.
31 I. P. S. Kapoor, P. Srivastava and G. Singh, *Propellants, Explos., Pyrotech.*, 2009, **34**, 351–356.
32 Y. F. Zhang, N. N. Wang, Y. T. Huang, *et al.*, *Ceram. Int.*, 2014, **40**, 11393–11398.
33 K. C. Gupta and A. K. Sutar, *Coord. Chem. Rev.*, 2008, **252**, 1420–1450.
34 A. Choudhary, S. Kumari and S. Ray, *ACS Omega*, 2017, **2**, 6636–6645.
35 H. Feizi, F. Shiri, R. Bagheri, M. M. Najafpour, *et al.*, *Catal. Sci. Technol.*, 2018, 1–15.
36 R. Kitaura, G. Onoyama, H. Sakamoto, *et al.*, *Angew. Chem., Int. Ed.*, 2004, **43**, 2684–2687.
37 D. S. Wankhede, S. Hussain, N. Jadhav, *et al.*, *Chem. Sin.*, 2013, **4**(5), 79–85.
38 P. Paul, K. R. N. Bhowmik, S. Roy, *et al.*, *Polyhedron*, 2018, **151**, 407–416.
39 D. di Chimica, G. Ciamician and V. Selmi, *Chem. Soc. Rev.*, 2004, **33**, 410–421.
40 M. R. Chapman, S. E. Henkelis, N. Kapur, *et al.*, *ChemistryOpen*, 2016, **27**, 112–118.
41 G. R. Gavalas, C. Phichitkul and G. E. Voecks, *J. Catal.*, 1984, **88**, 54–64.
42 Y. Ding, F. Wang, Z. J. Ku, *et al.*, *Russ. J. Coord. Chem.*, 2009, **35**(5), 360–366.
43 M. Kondo, K. Nabari, T. Horiba, *et al.*, *Inorg. Chem. Commun.*, 2003, **6**, 154–156.